

## Comparing In-Plane Equivalent Shear Stiffness of Timber Diaphragms Retrofitted with Light and Reversible Wood-Based Techniques

Mirra, M.; Ravenshorst, G.J.P.; van de Kuilen, J.W.G.

**DOI**

[10.1061/\(ASCE\)SC.1943-5576.0000602](https://doi.org/10.1061/(ASCE)SC.1943-5576.0000602)

**Publication date**

2021

**Document Version**

Accepted author manuscript

**Published in**

Practice Periodical on Structural Design and Construction

**Citation (APA)**

Mirra, M., Ravenshorst, G. J. P., & van de Kuilen, J. W. G. (2021). Comparing In-Plane Equivalent Shear Stiffness of Timber Diaphragms Retrofitted with Light and Reversible Wood-Based Techniques. *Practice Periodical on Structural Design and Construction*, 26(4), Article 04021031. [https://doi.org/10.1061/\(ASCE\)SC.1943-5576.0000602](https://doi.org/10.1061/(ASCE)SC.1943-5576.0000602)

**Important note**

To cite this publication, please use the final published version (if applicable). Please check the document version above.

**Copyright**

Other than for strictly personal use, it is not permitted to download, forward or distribute the text or part of it, without the consent of the author(s) and/or copyright holder(s), unless the work is under an open content license such as Creative Commons.

**Takedown policy**

Please contact us and provide details if you believe this document breaches copyrights. We will remove access to the work immediately and investigate your claim.

# **Comparing in-plane equivalent shear stiffness of timber diaphragms retrofitted with light and reversible wood-based techniques**

by

Michele Mirra, Geert Ravenshorst, Jan-Willem van de Kuilen

Published on ASCE Practice Periodical on Structural Design and Construction 26 (4), Nov. 2021

**[Link to original Open Access Article and Supplemental Material:](https://ascelibrary.org/doi/abs/10.1061/%28ASCE%29SC.1943-5576.0000602)**

<https://ascelibrary.org/doi/abs/10.1061/%28ASCE%29SC.1943-5576.0000602>

# Comparing in-plane equivalent shear stiffness of timber diaphragms retrofitted with light and reversible wood-based techniques

Michele Mirra<sup>1</sup>, Geert Ravenshorst<sup>2</sup>, Jan-Willem van de Kuilen<sup>3</sup>

<sup>1</sup>Ph.D. Candidate, Dept. of Engineering Structures, Delft University of Technology, 2628 CN Delft, The Netherlands.

(corresponding author). Email: [M.Mirra@tudelft.nl](mailto:M.Mirra@tudelft.nl)

<sup>2</sup>Assistant Professor, Dept. of Engineering Structures, Delft University of Technology, 2628 CN Delft, The

Netherlands. Email: [G.J.P.Ravenshorst@tudelft.nl](mailto:G.J.P.Ravenshorst@tudelft.nl)

<sup>3</sup>Professor, Dept. of Engineering Structures, Delft University of Technology, 2628 CN Delft, The Netherlands;

Professor, Dept. of Wood Technology, Technical University of Munich, 80797 Munich, Germany. Email:

[vandekuilen@hfm.tum.de](mailto:vandekuilen@hfm.tum.de)

**Abstract:** In-plane behavior of timber diaphragms is usually characterized by means of an equivalent shear stiffness. However, this value depends on how the stiffness of the floors is evaluated from the experimental tests. Although an increasing number of research studies provided a deeper insight into the seismic characterization of as-built and retrofitted timber diaphragms, the use of different standards or assumptions led to inhomogeneous and not comparable results. With a focus on light, reversible, wood-based strengthening techniques applied to existing diaphragms, in this work a uniform and simple method is proposed, based on the calculation of the secant stiffness of the floors at reference drifts. By means of this procedure, relevant research studies from literature were compared, and homogeneous, indicative values of equivalent shear stiffness were proposed for each considered strengthening technique. These results can contribute to a more aware and reliable use, design, and linear modelling of wood-based retrofitting solutions for existing timber diaphragms.

## Introduction

Existing or historical constructions with timber floors and roofs represent a significant part of the building stock and the architectural heritage for several countries. These diaphragms are often poorly connected to unreinforced masonry walls (Hsiao and Tezcan 2012), making such existing buildings potentially vulnerable to earthquakes. Depending on the specific contexts, the variety of construction methods and configurations of diaphragms led to a number of research studies focusing on the assessment of the seismic response of the floors and the development of retrofitting methods. Several Authors (Peralta et al. 2004; Corradi et al. 2006; Parisi and Piazza 2007; Piazza et al.

2008; Valluzzi et al. 2008; Baldessari 2010; Valluzzi et al. 2010; Brignola et al. 2012; Giongo et al. 2013; Wilson et al. 2014; Branco et al. 2015; Gubana and Melotto 2018; Mirra et al. 2020) emphasized the often poor characteristics in terms of in-plane strength and stiffness of as-built diaphragms, and proposed different refurbishment techniques. Among innovative options such as use of fiber-reinforced polymers (FRP) (Corradi et al. 2006; Piazza et al. 2008) or cross-laminated timber (CLT) (Branco et al. 2015; Gubana and Melotto 2018), all research studies also focused on light and reversible strengthening systems, due to their wide versatility and applicability in existing buildings, from houses to monumental constructions. In the recent years, these outcomes have provided new available information about the use and the effectiveness of such retrofitting methods.

In this framework, an important role is played by the increase in the floors in-plane stiffness gained with these refurbishments. This increase may ensure in existing buildings a better box-like behavior against seismic actions. However, it is difficult, if even not possible, to compare for the available research studies the in-plane stiffness of diaphragms with similar characteristics, or refurbished by means of the same technique (Giongo et al. 2018). This is primarily due to the different evaluation methods proposed in the standards adopted for calculating in-plane stiffness (EN 12512 2001; ASTM E 519-81 2002; FEMA 273 1997; FEMA 356 2000). Yet, even when following the same standard, inhomogeneity in Authors' assumptions can lead to not comparable outcomes. Therefore, given the importance of the correct evaluation of in-plane properties of timber diaphragms with a view to seismic performance of existing buildings, more homogeneous data would be greatly beneficial for characterizing the effectiveness of a certain retrofitting method. In fact, several studies highlighted the crucial role of in-plane stiffness of timber diaphragms in existing masonry buildings (Borri and Corradi 2018, Giongo et al. 2011, Gubana and Melotto 2021, Preti et al. 2017, Scotta et al. 2016, Scotta et al. 2017a, Scotta et al. 2017b, Scotta et al. 2018a, Scotta et al. 2018b, Trutalli et al. 2017, Trutalli et al. 2021), underlining that an excessive stiffening of the floors could even worsen their seismic performance. Therefore, an appropriate characterization of the in-plane response of timber diaphragms appears to be relevant and necessary for seismic assessment and retrofitting of existing masonry buildings.

The difficulty in comparing the available results from literature emerged when examining possible light, wood-based techniques to be adopted for strengthening timber diaphragms typical of the province of Groningen (NL), where human-induced earthquakes due to gas extraction occur. These events were unknown until recently: the gas extraction started in 1963, and earthquakes have occurred since the early '90s, with a progressive increase in the number of events and in their intensity. Up to now, the highest magnitude was recorded near Huizinge in 2012, and was equal to 3.6 on the Richter scale. The current building stock has not been designed to withstand seismic actions: nearly 50% of the buildings are composed of unreinforced single-leaf or double-wythe brick masonry walls, and light, flexible timber floors and roofs. The slenderness of the walls (both in-plane and out-of-plane) and the low in-plane

stiffness of the diaphragms, due to small-size timber members, make these existing buildings vulnerable against earthquakes (Messali et al. 2017). More specifically, these floors present light and slender structural elements: for instance, a main joist of a floor can have a cross section of 60×130 mm (or even 50×105 mm for a roof rafter), with large joists spacing, ranging from 600 to 900 mm. The floor sheathing is usually realized with continuous planks, having a thickness from 15 to 24 mm. Besides, roofs of detached houses are normally composed of main and secondary beams, connected with one nail at every intersection, and often poorly fastened to the walls (Mirra et al. 2020).

A literature survey was thus performed to evaluate possible reversible and effective retrofitting methods, and the opportunity to investigate simple and general criteria for comparing available results opened up when arranging an experimental campaign on the in-plane response of timber diaphragms with Dutch features at Delft University of Technology (Mirra et al. 2020). The criteria were formulated to more homogeneously compare the obtained test results with those present in literature, in order to better evaluate the performance and improvement of the applied refurbishment, given the high seismic vulnerability of existing Dutch floors. Since the adopted strengthening technique consisted of a plywood panels overlay (Mirra et al. 2020), only light, timber-based and reversible refurbishment methods for timber diaphragms were considered in the comparison.

The objective of this work is thus to summarize the main research studies on wood-based seismic retrofitting of timber floors, and to propose a simple, general method to compare the diaphragms stiffness in as-built and strengthened configurations. First, relevant studies are chosen for comparison, focusing on light and reversible wood-based retrofitting. Second, adopted standards for evaluating the in-plane stiffness of diaphragms are summarized, and a homogeneous procedure for comparison is proposed. It should be noticed that the present article does not question the validity of the present standards, but by making the different test results more comparable, tries to provide a more clear picture of the effectiveness and the improvement in stiffness gained with each retrofitting technique. Finally, the obtained homogenized data are discussed, and indicative stiffness values for light-strengthened diaphragms are provided.

## **Overview of Test Data on Diaphragms from Literature**

### **Summary of the Compared Diaphragms**

Fig. 1 provides an overview of the selected reference research studies on the in-plane response of diaphragms, and reports static schemes, dimensions and names of the samples, loading directions and adopted strengthening techniques: from this first summary, the variety of configurations is already evident. The order in which the samples are presented is according to the adopted strengthening techniques: superposition of an additional layer of planks

arranged at an angle of 45° (Valluzzi et al. 2008; Valluzzi et al. 2010) or at 90° (Corradi et al. 2006; Branco et al. 2015) with respect to the original sheathing; overlay of oriented strand board (OSB) panels (Gubana and Melotto 2018); overlay of plywood panels (Peralta et al. 2004; Brignola et al. 2012; Giongo et al. 2013; Wilson et al. 2014; Mirra et al. 2020). In the following sections, this same distinction among strengthening methods is adopted in presenting the configurations of the floors.

It is worth noticing that the experimental results in Piazza et al. (2008) and Baldessari (2010), although relevant for the subject, are not included in the comparison, due to the massive size of the structural elements, and because all tested diaphragms were surrounded by a continuous steel plate, fastened along the floor perimeter to simulate the presence of an improved connection to the masonry walls; this structural element remarkably increased the stiffness of the diaphragms, up to two times (Baldessari 2010). The chosen floors were, instead, strengthened with only timber-based techniques, and all similar, for each retrofitting method, in terms of structural elements size, and fasteners dimensions and position. Within this article, the main properties of the diaphragms are reported; for a comprehensive summary of all their characteristics, the reader is referred to the supplemental material, containing an exhaustive database useful for future studies.

## Equivalent Shear Stiffness

A common way to homogenize the stiffness values of timber diaphragms is to adopt a size-independent parameter, the equivalent shear stiffness ( $G_d = G \cdot t$ , with  $G$  floor's global shear modulus and  $t$  = thickness of the floor planking). It is important to underline that this parameter can be considered reliable for diaphragms for which the in-plane behavior can be assumed as shear-related, such as the strengthened ones; for as-built floors with continuous planks and joists, the flexural response is dominant, and hence  $G_d$  is size-dependent and loading direction dependent (Giongo et al. 2018). However, the equivalent shear stiffness was evaluated for as-built floors as well, in order to quantify, after strengthening them, their improvement compared to the initial conditions.

The equivalent shear stiffness  $G_d$  was derived for all diaphragms from their experimentally measured in-plane response and static scheme, with reference to their shear-related drift  $\gamma$  at the floors supports (Fig. 1):

$$G_d = \frac{V}{\gamma \cdot B} \quad (1)$$

In Eq. 1,  $V$  is the shear load acting on the floor according to its static scheme, while  $B$  is the length of the supported side of the floor, parallel to the in-plane load.

These calculations, reported in the coming sections, were in many cases also performed by the Authors. It should be noticed that, in this work, a comparison of only the stiffness of floors among several light wood-based retrofitting techniques will be given, but their potential energy dissipation will not be considered, since some of the reference

tests are monotonic and not cyclic. Should the reader be interested in investigating more the topic of the energy dissipation provided by (retrofitted) timber diaphragms, an overview and comparison of dissipative properties of floors strengthened with plywood panels is given in Mirra et al. (2021); other relevant studies in which the dissipative role of timber diaphragms in existing masonry buildings is discussed are, among others, Preti et al. (2017), Scotta et al. (2016), Scotta et al. (2017a), Scotta et al. (2017b), Scotta et al. (2018a), Scotta et al. (2018b), Trutalli et al. (2017), Trutalli et al. (2021).

## **Strengthening with a Superposition of Planks Arranged at an Angle of 45° with respect to the Original Sheathing**

**Valluzzi et al. (2008); Valluzzi et al. (2010)**

Valluzzi et al. (2008) and Valluzzi et al. (2010) present the same experimental campaign on timber floors, and the specimens are called *FMSB* and *FM*, or *F1.M* and *F2.M*, respectively. The static scheme for the horizontal loading and the main characteristics of the floors, shown in Fig. 2, are identical for both diaphragms; the only difference is in the choice of the planking: specimen *FMSB* (*F1.M*) presented straight-sheathed planks, while sample *FM* (*F2.M*) tongue-and-groove ones. The planks used for strengthening followed this same distinction, but tongue-and-groove ones were thicker with respect to the straight-sheathed ones (40 mm instead of 25). For a complete summary of the properties of the floors, the reader is referred to Table S1 of supplemental material.

The tests were performed in a vertical configuration, by means of a compact test setup. The aim of the tests was to study the behavior of a portion corresponding to 1/4 of a floor that could be found in practice. The Authors calculated the stiffness according to EN 12512 (2001), assuming as maximum force the value reached within 30 mm of displacement. Given the static scheme of Fig. 2, the equivalent shear stiffness for comparison in this paper is calculated as:

$$G_d = \frac{F \cdot L}{\delta \cdot B} = \frac{K \cdot L}{B} \quad (2)$$

In the former expression,  $F$  is the total applied load,  $L$  the span of the floor orthogonal to  $F$ ,  $B$  the restrained side of the floor (parallel to  $F$ ),  $\delta$  is the displacement corresponding to  $F$ , and  $K = F/\delta$  is the in-plane stiffness. For this floor,  $V = F$  and the shear-related drift is calculated as  $\delta/L$ .

## **Strengthening with a Superposition of Planks Arranged at an Angle of 90° with respect to the Original Sheathing**

### **Corradi et al. (2006)**

Corradi et al. (2006) tested both as-built and strengthened diaphragms. The only difference between the two as-built samples (specimens *01-T2-OR* and *02-T6-OR*) was in the number of the nails at each end of the planks: only one for sample *01-T2-OR*, three for specimen *02-T6-OR* (Fig. 3); the planks were 600 mm long. As a strengthening method, an overlay of 28-mm-thick planks arranged at an angle of 90° with respect to the original sheathing was then applied in specimen *03-T4-T6*, but for this case the planks were connected with two nails at each end. For a deeper overview of the properties of the floors, see Table S2 in supplemental material.

The test represented a half of the floor and the setup allowed to apply the load in a single point. For these floors, the Authors evaluated the stiffness by means of the formulation in ASTM E 519-81 (2002), applied for the analysis of their shear behavior. Given the static scheme of Fig. 3, the equivalent shear stiffness for comparison in this paper is calculated according to Eq. 2, with  $V = F$  and the shear-related drift determined as  $\delta/L$  as well.

### **Branco et al. (2015)**

J. M. Branco et al. (2015) tested one as-built floor (specimen *S*) and, among other samples, specimen *SS*, consisting of a diaphragm strengthened with an overlay of 20-mm-thick planks arranged at an angle of 90° with respect to the original sheathing. In Fig. 4 the static scheme and the main characteristics of the tested floors are shown; a deeper overview of their properties is given in Table S3 of supplemental material.

The Authors calculated the stiffness of the floors using the same procedure reported in EN 12512 (2001), but with reference to EN 26891 (1991), since the tests were monotonic and not cyclic in this specific case. The Authors did not assume the maximum force as the absolute highest value reached during the test, but as the maximum recorded load within the interval 0-100 mm.

Given the static scheme of Fig. 4, the equivalent shear stiffness for comparison in this paper is calculated according to Eq. 2;  $V = F$  and the shear-related drift is determined as  $\delta/L$ .

## **Strengthening with an Overlay of OSB Panels**

### **Gubana and Melotto (2018)**

A. Gubana and M. Melotto (2018) analyzed the response of as-built floors, and tested (among others) the performance of specimens retrofitted with 25-mm-thick OSB panels. Fig. 5 shows the as-built sample (*UR-2*) and the two strengthened ones considered (*OSB90-R-2*, with panels oriented orthogonal to joists, and *OSB0-S-2*, with panels

arranged parallel to joists). Detailed information on the diaphragms properties can be found in Table S4 of supplemental material.

The Authors evaluated the stiffness of the floors according to EN 12512 (2001). Given the static scheme of Fig. 5, the equivalent shear stiffness for comparison in this paper is calculated according to Eq. 2, with  $V = F$  and the shear-related drift determined as  $\delta/L$  as well.

## Strengthening with an Overlay of Plywood Panels

### Peralta et al. (2004)

Peralta et al. (2004) tested a number of flexible floors and studied several strengthening techniques. Among the tested samples, specimens *MAE-2* is analyzed in this section. The strengthening technique consisted of unblocked or blocked 9.5-mm-thick plywood panels overlay, tested in samples *MAE-2B* and *MAE-2C*, respectively. In the unblocked configuration the panels were fastened with nails only to the existing sheathing and the joists. In the blocked configuration, additional timber elements were placed in between the joists, in correspondence to the panels edges, and the panels were nailed through the sheathing to them; additional fasteners were also used, compared to the unblocked configuration (Peralta et al. 2004). The main characteristics of the diaphragm, as well as its static scheme, are reported in Fig. 6. To laterally support the joists, cross-bridging members were also present to reproduce the characteristics of pre-1950 diaphragms realized in the US. Bridging was typically made of short wood boards that were set nailed diagonally between joists to form an “X” pattern perpendicular to them. In this case, the specimens featured two rows of bridging elements, placed at 1220 mm from the floor edges, and with a cross section of 38x89 mm. Additional information on the floors properties can be found in Table S5 of supplemental material.

The floor was tested in a horizontal configuration and was subjected to an in-plane load applied in two points at  $L/3$  from the supports. The Authors calculated the stiffness of the floor according to the bilinear representation reported in FEMA 273 (1997). After the evaluation of the experimental stiffness with this method, the Authors also compared this value with the one that could be predicted by both FEMA 273 (1997) and FEMA 356 (2000) guidelines, according to the standardized parameters reported there; the Authors underlined that the stiffness prediction in agreement with these standards was not so accurate.

Given the static scheme of Fig. 6, the equivalent shear stiffness for comparison in this paper is calculated as follows:

$$G_d = \frac{F \cdot L}{6 \cdot \delta \cdot B} = \frac{K \cdot L}{6 \cdot B} \quad (3)$$

For this floor,  $V = F/2$ ,  $L = 7320$  mm and the shear-related drift is determined as  $\delta/(L/3)$ .

### **Brignola et al. (2012)**

Brignola et al. (2012) tested a series of flexible and refurbished timber floors in order to characterize their properties for the New Zealand building context. In this section, as-built specimen *AB-1* and its strengthened version *R-1*, are discussed. The retrofitting consisted of an overlay of 19-mm-thick plywood panels. The static scheme and the characteristics of the floors are reported in Fig. 7; for a detailed overview see Table S6 in supplemental material.

The floor was subjected to a load applied in two points at  $3L/8$  from the supports, and the test was performed in agreement with EN 12512 (2001). The Authors evaluated the stiffness of the floor as the secant value at 12 mm of displacement, and at the maximum displacement reached during the test. Given the static scheme in Fig. 7, the equivalent shear stiffness for comparison in this paper is calculated as follows:

$$G_d = \frac{3 \cdot F \cdot L}{16 \cdot \delta \cdot B} = \frac{3 \cdot K \cdot L}{16 \cdot B} \quad (4)$$

For this floor,  $V = F/2$ ,  $L = 4000$  mm and the shear-related drift is determined as  $\delta/(3L/8)$ .

### **Giongo et al. (2013)**

Giongo et al. (2013) tested two vintage timber floors in situ. These diaphragms had typical characteristics from the New Zealand context: the structural elements were made of native wood species (Rimu and Matai), and the joists presented a large height-to-width ratio. Additionally, 50-mm-thick timber blocking elements were placed on the floors supported edges, to improve the otherwise poor connection to masonry. Cyclic tests were carried out on different configurations: in this case, the as-built floor was designated as sample *26\_B\_asB*, and then it was strengthened with plywood panels screwed on the existing sheathing (specimen *35\_B\_Plyw*). The arrangement of the plywood panels was chosen aiming at creating an interlocking effect, to reduce a possible orthotropic response. The static scheme and the floor's characteristics are reported in Fig. 8: to ensure an appropriate lateral support to the joists, the floor presented also cross-bracing elements between the joists, at 1.5 m spacing. The in-situ testing apparatus was arranged in such a way that it was possible to apply an horizontal load in four points, simulating a parabolic distribution of the force. For further information on the diaphragms properties, see Table S7 of supplemental material. In the publication (Giongo et al. 2013), the equivalent shear stiffness is given directly, according to the static scheme of Fig. 8:

$$G_d = \frac{F \cdot \left(a + \frac{b}{2}\right)}{2 \cdot \delta \cdot B} = \frac{K \cdot \left(a + \frac{b}{2}\right)}{2 \cdot B} \quad (5)$$

where  $a$  is the distance from the side of the diaphragm to the first point of application of the load and  $b$  is the distance between the first and the second point of application of the load (in this case,  $L/8$  and  $L/4$ , respectively). The other quantities have the same meaning of those reported in the previous sections; for this floor,  $V = F/2$  and the shear-

related drift is determined as  $\delta/(L/4)$ . It should be noticed that the Authors considered as drift the ratio between the midspan in-plane displacement and half of the floor span. This corresponds to half of the shear-related drift, and was taken into account in the comparison as well.

#### **Wilson et al. (2014)**

Wilson et al. (2014) tested a series of as-built and refurbished timber floors in order to study their orthotropic behavior. These analyses were conducted to obtain the value of in-plane stiffness for the same diaphragm loaded in both directions. Therefore, two as-built specimens (*1a-PARA* and *1a-PERP*), and two samples strengthened with 15-mm-thick plywood panels (*1b-PARA* and *1b-PERP*), were tested parallel and perpendicular to the joists, as shown in Figs. 9 and 10. The floors were subjected to a horizontal load applied in four points (specimens *1a-PARA* and *1b-PARA*) or two points (specimens *1a-PERP* and *1b-PERP*). In order to ensure the stability of the floors, at 1845 mm heart-to-heart distance a 45x75 mm cross-bracing system was positioned for specimen *1a-PARA*, while for sample *1a-PERP* this was substituted with blocks having the same cross-section as the main joists. For further information on the diaphragms properties, see Table S8 of supplemental material.

The Authors calculated the stiffness of the non-strengthened floors according to the bilinear method proposed in FEMA 273, adopted also by Peralta et al. (2004). On the contrary, for the strengthened diaphragms ASTM E 2126 (2019) was followed, which is also based on the hysteretic energy conservation principle, but it proposes an elastic–perfectly plastic bilinear representation, more suitable for the obtained load-displacement curves.

Given the static scheme in Fig. 9, the equivalent shear stiffness for specimens *1a-PARA* and *1b-PARA* is calculated again with Eq. 5 ( $a = 3L/13$  and  $b = 5L/26$ ), with  $V = F/2$  and the shear-related drift defined as  $\delta/(17L/52)$ . Instead, according to Fig. 10, the equivalent shear stiffness for specimen *1a-PERP* and *1b-PERP* is calculated as follows:

$$G_d = \frac{F \cdot a}{2 \cdot \delta \cdot B} = \frac{K \cdot a}{2 \cdot B} \quad (6)$$

For these two specimens,  $V = F/2$  and the shear-related drift is determined as  $\delta/a$ , with  $a = 1.71$  m (Wilson et al. 2014).

#### **Mirra et al. (2020)**

This testing campaign triggered the attempt of a more general comparison among wood-based retrofitting techniques. Five diaphragms with Dutch features were tested in both as-built and strengthened configurations. Two floors were tested parallel to the joists (samples *DFpar-1* and *DFpar-2*, Fig. 11), two perpendicular to the joists (samples *DFper-3* and *DFper-4*, Fig. 12) and one was representative for a roof pitch, loaded parallel to the purlins (sample *DRpar-5*, Fig. 13). Sample *DFpar-2* had thicker planks compared to the other diaphragms (24 mm instead of 18 mm). Specimens *DFper-3* and *DFper-4* were identical, but two configurations were considered at the joists ends: a hinged one for sample *DFper-3*, simulating a joists ending in a masonry pocket without mortar; a clamped one for specimen *DFper-*

4, reproducing a slightly better condition with the joists ends fully surrounded by mortar (Mirra et al. 2020; Fig. 12). These two configurations did not show significant differences in in-plane response.

The same specimens were then strengthened with 18-mm-thick plywood panels and tested again (samples *DFpar-1s*, *DFpar-2s*, *DFper-3s*, *DFper-4s*, *DRpar-5s*). In addition to the plywood panels overlay, for sample *DFper-4s* 60-mm-thick timber blocking elements were placed at the top of the diaphragm between the joists, to improve the shear transfer and simulate a connection to the masonry walls, similarly to the aforementioned tests of Giongo et al. (2013); for sample *DRpar-5s* the base roof connection was improved with steel angles. Further details are reported in Tables S9, S10 and S11 of supplemental material.

The setup and the testing protocol were developed according to ISO 21581 (2010). The diaphragms were tested in a vertical configuration representing a half of a real floor (or one pitch in the case of the roof). The stiffness of the floors was calculated at reference drifts: given the static schemes shown in Figs. 11 to 13,  $G_d$  is calculated according to Eq. 2,  $V = F$  and the drift is determined as  $\delta/L$ .

## Methods for the Calculation of In-plane Stiffness

### General

In the previously presented research studies, the Authors adopted different standards to determine the in-plane stiffness and strength of timber diaphragms. The inhomogeneity in available data does not only depend on the different contexts or standards (from testing protocols to stiffness calculations), but is also related to Authors' assumptions, leading to not uniform results. In the following sections, these standards will be summarized and a simple and homogeneous comparison method will be proposed.

### Standards Adopted in the Reported Research Studies

#### EN 12512 (2001)

Although this standard is intended for connections, in the European context EN 12512 (2001) is often adopted also for the calculation of the in-plane stiffness of timber floors. According to this formulation, the stiffness is calculated after determining a conventional yielding point on the experimental load-displacement backbone curve; two different methods are proposed:

- If the load-displacement curve is clearly defined by two linear parts, then the yielding point is found as the intersection of the lines tangent to these two branches;
- When the load-displacement curve is not composed of two linear parts, after defining the maximum load  $F_{max}$ , the yielding point is found as the intersection of two lines defined as follows: the first one intersects the two points on the load-displacement curve corresponding to  $0.1F_{max}$  and  $0.4F_{max}$ , while the second one is

the line tangent to the load-displacement curve, having a slope of 1/6 with respect to the first one. This procedure almost always applies to describe the seismic response of timber diaphragms, due to their usual nonlinearity.

The main issue of this formulation is related to the choice of the value of  $F_{max}$  for flexible diaphragms: in fact, while for instance Piazza et al. (2008) and Gubana and Melotto (2018) refer to the entire load-displacement curve, Valluzzi et al. (2008) and Branco et al. (2015) consider also the fact that the maximum force should not correspond to a too large value of displacement, which would imply an out-of-plane collapse of the masonry walls supporting the floor in an existing building. Therefore, the value of  $F_{max}$  to be chosen in this second case should not be the absolute maximum one, but the highest level of load in an acceptable displacement range.

#### **ASTM E 519-81 (2002)**

This standard was developed as a guideline for experimental set-up and interpretation of the diagonal compression test on masonry, in order to evaluate its shear strength. In the case of timber floors, the same procedure to determine the secant stiffness at 1/3 of the maximum load was applied by Corradi et al. (2006).

A description of the behavior of the floor in the plane is supplied by the function relating the applied shear force  $V$  and the resulting displacement  $\delta$ :

$$V = K\delta \cong k(\gamma L) \quad (7)$$

in which  $\gamma$  is the floor's angular strain. The shear stiffness corresponds to the secant value at 1/3 of the maximum load on the envelope curve of the loading cycles:

$$k_{1/3} = \frac{V_{1/3}}{\gamma_{1/3}L} \quad (8)$$

The angular strain is calculated by referring to the compression and traction strains associated with the diagonal measurements of the floor.

#### **FEMA 273 (1997), FEMA 356 (2000) and ASTM E 2126 (2019)**

The FEMA guidelines are both reported because they were adopted by Peralta et al. (2004), but currently FEMA 356 (2000) replaced FEMA 273 (1997); ASTM E 2126 (2019) was instead referred to in Wilson et al. (2014). For all three cases, the formulation consists of the definition of a simplified bilinear backbone curve that approximates the actual one: this equivalent bilinear system is found in such a way that it presents the same energy absorption of the real system, and this determines the initial stiffness as well. While for FEMA guidelines the bilinear curve has a hardening phase, for ASTM E 2126 it is elastic-perfectly plastic (Fig. 14).

## Proposed Evaluation Method

Brignola et al. (2012), Giongo et al. (2013), and Mirra et al. (2020) did not follow specific standardized procedures for the evaluation of the in-plane stiffness of timber floors. The assumption was to calculate the value of stiffness intersecting the floor's backbone curve at a certain drift level: this method appears to be immediate and also more useful to compare all the obtained results, because it is simple, uniform, and can be applied at different drifts. Besides, from the experimental data no influence of initial stages with low stiffness due to e.g. presence of gaps was noticed. This procedure appeared thus to be suitable for comparison, and is proposed to derive stiffness values from the experimental results at defined drifts, for both as-built and strengthened floors.

After this first step, the values are homogenized by adopting the equivalent shear stiffness  $G_d$ . This parameter is suitable to characterize retrofitted diaphragms, because they exhibit a more shear-related behavior. For as-built floors, especially when continuous planks and joists are present, the flexural response can be dominant and hence  $G_d$  cannot be considered size-independent or direction-independent (Giongo et al. 2018). Nevertheless, the equivalent shear stiffness was always calculated also for the as-built floors, in order to compare them to the strengthened ones.

If it is possible to make the results uniform and comparable in terms of stiffness, then also  $G_d$  can be a reliable and representative value for a certain strengthening technique. However, this equivalent shear stiffness is still drift-dependent, and can also be influenced by the loading direction (Wilson et al. 2014; Mirra et al. 2020). Both nonlinear and orthotropic behavior was therefore taken into account when comparing the diaphragms.

In the following section the values of stiffness and  $G_d$  are reported, as derived from the experimental results by the different Authors. These values were then recalculated with reference to specific drift levels, fixed for all of them, in order to make these results comparable. Given the particular situation in the region of Groningen, subjected to induced earthquakes, a limited deflection of the diaphragms is expected, but can already be detrimental for local unreinforced masonry structures, due to the large slenderness of the walls and the frequent presence of poor-quality masonry. Therefore, for the results reported in Mirra et al. (2020) stiffness of the diaphragms was evaluated at a very initial phase (0.10% drift) and at a higher but not excessive level of drift (1.00%), when nonlinear behavior is dominant. Thus, these same drift limits were adopted for comparison with the other reported reference tests. Additionally, a third value of stiffness was calculated, with reference to a conventional yielding point of the floor: this was defined as the intersection between the following two lines (Fig. 15):

- An initial stiffness, determined according to EN 12512 (2001), and taking as  $F_{max}$  the value of total in-plane load at 1.00% drift;
- The tangent to the experimental curve determined at the maximum considered drift of 1.00%.

It should be noticed that other reference drift values for calculating the secant stiffness could also be adopted; in this study it was chosen to examine a range that is of interest for the Dutch context. All values of stiffness were calculated based on the graphs and hysteretic cycles available in each reference publication.

## Analysis

### General

In the various reported studies, as-built diaphragms displayed in general a very flexible response, and for certain configurations the floors were almost not able to withstand in-plane loads without large deformations (samples *FMSB*, *FM*, *S*, *UR-2*, *DRpar-5*), especially due to low rotational stiffness of the nail couples. Furthermore, an orthotropic response was observed when considering the two directions of loading (samples *1a-PARA*, *1a-PERP*, *DFpar-1*, *DFpar-2*, *DFper-3*, *DFper-4*). This property of floors has therefore to be considered, when modelling them with the purpose of the assessment of an existing building's seismic performance.

Table 1 summarizes the values of stiffness calculated by the Authors and with the proposed method for each research study; in the table, as-built (original) samples are identified by letter (*O*), strengthened ones by letter (*S*), and their names are according to the notation used by the Authors. It should be noticed that, since for several as-built floors  $G_d$  is size-dependent, a comparison between original and strengthened diaphragms is either possible for the same Authors, or for floors having similar dimensions or aspect ratio. Instead, the equivalent shear stiffness values of strengthened diaphragms can be compared among each other, due to their more shear-related response. This comparison is illustrated in the following section.

### Comparison among the Strengthened Diaphragms

#### Introduction

Unlike as-built samples, the shear-related behavior of strengthened diaphragms allows to calculate for all of them an equivalent shear stiffness that can be considered more size-independent, enabling their comparison. Fig. 16 shows the calculated  $G_d$  values for all strengthened floors at reference drifts. The obtained results are discussed in the following, by distinguishing among the strengthening techniques.

#### **Strengthening with a Superposition of Planks Arranged at an Angle of 45° with respect to the Original Sheathing**

Specimens *FM+45°SP(A)* and *FM+45°SP(B)* displayed approximately the same stiffness, thus the influence of friction among planks in the in-plane response becomes less evident, contrarily to the as-built case (Table 1). Planks placed at an angle of 45° enabled a large improvement in the in-plane stiffness, up to more than 10 times compared to the original samples.

### **Strengthening with a Superposition of Planks Arranged at an Angle of 90° with respect to the Original Sheathing**

Sample *03-T4-T6* displayed a very high stiffness at initial stages, while at larger drifts a reduction until a value in line with other floors is observable. This response could depend on the floor's structure as well, characterized by a double warping of main and secondary joists. Specimen *SS* showed the lowest stiffness: a superposition of planks arranged orthogonally with respect to the existing sheathing is thus (as expected) less effective compared to arranging the boards at an angle of 45°: the in-plane stiffness could be increased by up to 4 times. On average, it can be concluded that  $G_d$  is approximately 1.5 to 2 times higher for the former strengthening with respect to the latter.

### **Strengthening with an Overlay of OSB Panels**

Floors *OSB90-R-2* and *OSB0-S-2* show the influence of the direction in which OSB panels are arranged with respect to the sheathing. With panels placed perpendicular to the joists only half of the stiffness is obtained at every reference drift with respect to the configuration having panels positioned parallel to the joists. In any case, the improvement in in-plane stiffness is considerable compared to the as-built situation (Table 1), with an increase of approximately 5 and 10 times for panels arranged perpendicular and parallel to the joists, respectively.

As noticeable from Fig. 16, this technique can be considered equivalent to the plywood panels overlay (see next section). Thus, similarly to a plywood panel retrofitting, the arrangement of OSB panels could be optimized in order to make the floor isotropic after strengthening, similarly to the aforementioned interlocked overlay proposed by Giongo et al. (2013).

### **Strengthening with an Overlay of Plywood Panels**

Strengthening with plywood panels appears to give similar results in terms of shear stiffness, at least for floors having a total sheathing thickness (very common in practice) between 30 and 40 mm, like the considered ones.

Unblocked and blocked plywood panels, present in sample *MAE-2B* and *MAE-2C*, respectively, could be both recommendable interventions depending on the specific situation: in the latter case, the stiffness is doubled compared to the former strengthening option. Specimen *R-1* was strengthened with an unblocked plywood panels overlay as well, and the value of stiffness is thus similar to floor *MAE-2B*.

The same observation can be made for samples *1b-PARA* and *1b-PERP*, even if an orthotropic behavior is present, with a lower stiffness for the direction perpendicular to the joists. On the contrary, in floor *35\_B\_Plyw*, also tested orthogonally to the joists, the more interlocked plywood panels overlay, along with the presence of the timber blocking elements at the floor edges, an increased stiffness was obtained, which is very close to that of specimens tested parallel to the joists. Therefore, the orthotropic behavior is in this case fully mitigated.

The diaphragms tested by Mirra et al. (2020) reflected all the values obtained when strengthening with an unblocked plywood panels overlay, including again the orthotropic response, detected in sample *DFper-3s*. The only exception is represented by specimen *DFper-4s* that can be regarded as an example of partially blocked panels overlay: the blocks were placed between the joists at their end supports, similarly to the intervention realized by Giongo et al. (2013). The floor strengthened in this way, and tested perpendicular to the joists, showed in-plane stiffness values comparable to the ones tested parallel to the joists. Furthermore, it was possible to double its stiffness with respect to the unblocked sample *DFper-3s* as well, thus confirming the results obtained by Wilson et al. (2014) with samples *1b-PARA* and *1b-PERP*. Even the roof sample *DRpar-5s* displayed a great improvement, especially when compared to the as-built situation (Table 1): this proves once more the effectiveness of the plywood panels overlay as a retrofitting technique, because even Dutch timber diaphragms with small and light structural elements are able to reach in-plane stiffness values that are comparable to those of all other reported floors.

Summarizing, a remarkable improvement in stiffness can be gained when fully blocking the panels (sample *MAE-2C*), from 1.5 to 2 times compared to an unblocked overlay. This difference appeared also when loading the floors perpendicular to the joists, with a doubled stiffness when ensuring an efficient shear transfer at the floor supports with timber blocks (samples *35\_B\_Plyw* and *DFper-4s*). In general, considering an unblocked plywood panels overlay, but with timber blocks at the edges, the floors can thus be treated as isotropic. When loading perpendicular to the joists, these values are halved if timber blocks are not present. This is a further demonstration of how important the role of boundary conditions (connections to masonry walls, presence of other non-structural elements, thickness and size of plywood panels, etc.) can be.

## **Reference Equivalent Shear Stiffness Values for Seismic Analysis of Existing Buildings**

In Fig. 17 reference values of the stiffness of the tested retrofitted floors are reported, classifying them according to the adopted strengthening technique; correlations that emerged from the compared values are presented as well. These values were calculated by considering an average of those referred to each experimental test on the presented wood-based techniques.

Within the framework of the seismic assessment and retrofitting of existing buildings with timber diaphragms, the following recommendations can be made:

- When considering as-built floors, the use of size-independent or direction-independent values of  $G_d$  might not be suitable to represent the actual stiffness of the diaphragms, especially when their flexural deflection is dominant. In these cases, the floors stiffness can be determined by considering the flexural properties of planks or joists, depending on the loading direction (Mirra et al. 2020);

- When considering retrofitted floors, the use of  $G_d$  is more appropriate, and with a proper design of the retrofitting interventions, the behavior of the diaphragms could become isotropic;
- For seismic analyses at serviceability limit state, use of the values at 0.1% drift (or at yielding) is advised, while at near-collapse limit state it is recommended to adopt the values at 1.0% drift, which can account for the nonlinear response of the (retrofitted) diaphragms.

## Conclusions

This work proposed a simple and general method to compare test results, selected from literature, in terms of in-plane stiffness of timber floors strengthened with light, reversible wood-based techniques. Therefore, for the four considered retrofitting methods, homogeneous reference values for the equivalent shear stiffness were calculated and compared. In this way, it is possible to more accurately and reliably analyze the impact of the refurbishment of the floors on the global seismic response of existing buildings. In general, for as-built floors the behavior can be strongly orthotropic and either flexural or shear-related; for refurbished diaphragms, all the examined wood-based techniques showed to improve their in-plane response. The following key aspects resulted of particular importance:

- Comparing the equivalent shear stiffness values as the various Authors calculate them is not possible, due to the different methods adopted. For this reason, the secant stiffness at reference drift levels was calculated for all the discussed tests, in order to make them comparable. This resulted in a lower variation and an increased homogeneity of the equivalent shear stiffness values for the same retrofitting technique;
- When retrofitting with OSB and plywood panels, the differences in stiffness between the two directions of the floors can be strongly smoothed or eliminated when ensuring a proper blocking of the diaphragm's edges between the joists. Also the way the overlay is arranged, for both planks and panels, can have a great impact on the final floor's stiffness.
- It is recommended to characterize diaphragms not only with a single value of equivalent shear stiffness, but also accounting for the expected level of drift reached: for instance, values at 0.1% and 1.0% in-plane drift were in this case provided, to describe both linear and nonlinear response. A further process of harmonization of the methods to assess the equivalent shear stiffness is therefore recommendable as well.
- Retrofitting existing diaphragms with an overlay of planks arranged at 45° with respect to the existing sheathing could provide an increase in in-plane stiffness of up to 10 times compared to that of the original floors. Reference equivalent in-plane stiffness values of  $G_d = 2000$  N/mm (0.1% drift) and  $G_d = 700$  N/mm (1.0% drift) can be assumed for this strengthening technique, when conducting seismic analyses at serviceability limit state, or near-collapse limit state, respectively.

- Strengthening existing diaphragms with a superposition of planks arranged at 90° with respect to the existing sheathing could provide an increase in in-plane stiffness of up to 4 times compared to that of the original floors. Reference equivalent in-plane stiffness values of  $G_d = 600$  N/mm (0.1% drift) and  $G_d = 170$  N/mm (1.0% drift) can be assumed for this retrofitting technique, when conducting seismic analyses at serviceability limit state, or near-collapse limit state, respectively.
- An overlay of OSB panels arranged orthogonal to the existing joists could provide an increase in in-plane stiffness of more than 5 times compared to that of the original floors. Reference equivalent in-plane stiffness values of  $G_d = 2700$  N/mm (0.1% drift) and  $G_d = 600$  N/mm (1.0% drift) can be assumed for this strengthening technique, when conducting seismic analyses at serviceability limit state, or near-collapse limit state, respectively. If the panels are placed parallel to the joists, values of  $G_d = 5300$  N/mm (0.1% drift) and  $G_d = 1200$  N/mm can be assumed.
- An overlay of plywood panels could provide an increase in in-plane stiffness of up to 10 times compared to that of the original floors. For an unblocked overlay, reference equivalent in-plane stiffness values of  $G_d = 3400$  N/mm (0.1% drift) and  $G_d = 1300$  N/mm (1.0% drift) can be assumed for this strengthening technique, when conducting seismic analyses at serviceability limit state, or near-collapse limit state, respectively. If timber blocking elements are present to improve the shear transfer at the floors edges, the diaphragm can be considered as isotropic; otherwise, for the loading direction orthogonal to the joists, an orthotropic behavior should be considered, and lower values of  $G_d = 1300$  N/mm (0.1% drift) and  $G_d = 700$  N/mm (1.0% drift) can be assumed. If the panels overlay is fully blocked, values of  $G_d = 6000$  N/mm (0.1% drift) and  $G_d = 1700$  N/mm can be assumed.

The overview presented in this paper can provide guidance and more insight into a proper choice of timber-based strengthening solutions, and the reported values can serve as a more reliable input for a preliminary seismic assessment or design of these retrofitting interventions when improving the global structural response to earthquakes of existing buildings.

## Data Availability Statement

All data, models, and code generated or used during the study appear in the submitted article.

## **Acknowledgments**

The authors thankfully acknowledge NAM (*Nederlandse Aardolie Maatschappij*) for the financial support given to this study.

## **Supplemental Material**

Tables S1-S11 are available online in the ASCE Library ([ascelibrary.org](http://ascelibrary.org)).

## References

- Applied Technology Council (ATC). 1997. *NEHRP guidelines for the seismic rehabilitation of buildings*. FEMA Publication 273, Building Seismic Safety Council, Washington, D.C.
- ASCE. 2000. *Prestandard and commentary for the seismic rehabilitation of buildings (FEMA 356)*. Prepared for FEMA. Reston, VA: ASCE.
- ASTM. 2002. *Standard Test Method for Diagonal Tension (Shear) in Masonry Assemblages*. ASTM E 519-81. West Conshohocken, PA: ASTM.
- ASTM. 2019. *Standard Test Methods for Cyclic (Reversed) Load Test for Shear Resistance of Vertical Elements of the Lateral Force Resisting Systems for Buildings*. ASTM E 2126-19. West Conshohocken, PA: ASTM.
- Baldessari, C. 2010. "In-plane Behaviour of Differently Refurbished Timber Floors." Ph.D. Dissertation, University of Trento.
- Borri, A., and M. Corradi. 2018. "Structural Engineers vs. Conservators, Safety vs. Preservation: Problems, Doubts and Proposals." 1<sup>st</sup> International Conference TMM\_CH: Transdisciplinary Multispectral Modelling and Cooperation for the Preservation of Cultural Heritage, Athens, Greece.
- Branco, J. M., M. Kekeliak, and P.B. Lourenço. 2015. "In-Plane Stiffness of Timber Floors Strengthened with CLT." *Eur. J. Wood Wood Prod.* 73, 313-323.
- Brignola, A., S. Pampanin, and S. Podestà. 2012. "Experimental Evaluation of the In-Plane Stiffness of Timber Diaphragms." *Earthquake Spectra* 28(4), 1–23.
- CEN (European Committee for Standardization). 1991. *Timber Structures – Joints Made with Mechanical Fasteners – General Principles for the Determination of Strength and Deformation Characteristics*. EN 26891. CEN, Brussels, Belgium.
- CEN (European Committee for Standardization). 2001. *Timber Structures – Test Methods – Cyclic Testing of Joints Made with Mechanical Fasteners*. EN 12512. Brussels, Belgium: CEN.
- Corradi, M., E. Speranzini, A. Borri, and A. Vignoli. 2006. "In-Plane Shear Reinforcement of Wood Beam Floors With FRP." *Composites: Part B* 37, 310-319.

Giongo, I., M. Piazza, and R. Tomasi. 2011. "Pushover analysis of traditional masonry buildings: influence of refurbished timber-floors stiffness." SHATIS'11 International Conference on Structural Health Assessment of Timber Structures, Lisbon, Portugal.

Giongo, I., D. Dizhur, R. Tomasi, and J. M. Ingham. 2013. "In-plane assessment of existing timber diaphragms in URM buildings via quasi-static and dynamic in-situ tests." *Advanced Materials Research* 778, 495-502.

Giongo, I., E. Rizzi, J. M. Ingham, and D. Dizhur. 2018. "Numerical Modeling Strategies for In-Plane Behavior of Straight Sheathed Timber Diaphragms." *J. Struct. Eng.* 144 (10): 04018163. [https://doi.org/10.1061/\(ASCE\)ST.1943-541X.0002148](https://doi.org/10.1061/(ASCE)ST.1943-541X.0002148).

Gubana, A., and M. Melotto. 2018. "Experimental tests on wood-based in-plane strengthening solutions for the seismic retrofit of traditional timber floors." *Constr. Build. Mater.* 191, 290–299.

Gubana, A., and M. Melotto. 2021. "Discrete-element analysis of floor influence on seismic response of masonry structures." Proceedings of the Institution of Civil Engineers – Structures and Buildings. <https://doi.org/10.1680/jstbu.19.00099>

Hsiao, J.K. and J. Tezcan. 2012. "Seismic Retrofitting for Chord Reinforcement for Unreinforced Masonry Historic Buildings with Flexible Diaphragms". *Pract. Period. Struct. Des. Constr.* 17(3), 102-109.

International Organization for Standardization (ISO). 2010. *Timber Structures – Static and Cyclic Lateral Test Load – Test Methods for Shear Walls*. ISO 21581:2010. Geneva, Switzerland: ISO.

Messali, F., G.J.P. Ravenshorst, R. Esposito, and J.G. Rots. 2017. "Large-scale testing program for the seismic characterization of Dutch masonry walls". Proceedings of 16<sup>th</sup> World Conference on Earthquake (WCEE), Santiago, Chile.

Mirra, M., G.J.P. Ravenshorst, J.W.G. van de Kuilen. 2020. "Experimental and analytical evaluation of the in-plane behaviour of as-built and strengthened traditional wooden floors". *Eng. Struct.* 211 <https://doi.org/10.1016/j.engstruct.2020.110432>

Mirra, M., G.J.P. Ravenshorst, J.W.G. van de Kuilen. 2021. "Dissipative properties of timber diaphragms strengthened with plywood panels". Proceedings of the 16<sup>th</sup> World Conference on Timber Engineering, Santiago, Chile. (submitted)

Parisi, M.A., and M. Piazza. 2006. "Restoration and Strengthening of Timber Structures: Principles, Criteria, and Examples." *Pract. Period. Struct. Des. Constr.* 12(4), 177-185.

Peralta, D.F., M.J. Bracci, and M.B.D. Hueste. 2004. "Seismic Behavior of Wood Diaphragms in Pre-1950s Unreinforced Masonry Buildings." *J. Struct. Eng.* 130 (12), [https://doi.org/10.1061/\(ASCE\)0733-9445\(2004\)130:12\(2040\)](https://doi.org/10.1061/(ASCE)0733-9445(2004)130:12(2040)).

Piazza, M., C. Baldessari, and R. Tomasi. 2008. "The Role of In-Plane Floor Stiffness in the Seismic Behaviour of Traditional Buildings." 14<sup>th</sup> World Conference on Earthquake Engineering, Beijing, China.

Preti, M., S. Loda, V. Bolis, S. Cominelli, A. Marini, and E. Giuriani. 2017. "Dissipative roof diaphragm for the seismic retrofit of listed masonry churches". *J. Earthq. Eng.* 23(8), 1241–1261.

Scotta, R., D. Trutalli, L. Marchi, and L. Pozza. 2016. "Effects of in-plane strengthening of timber floors in the seismic response of existing masonry buildings." World Conference on Timber Engineering, Vienna, Austria.

Scotta, R., D. Trutalli, L. Marchi, L. Pozza, and M. Mirra. 2017. "Seismic response of masonry buildings with alternative techniques for in-plane strengthening of timber floors." *Revista Portuguesa de Engenharia de Estruturas*, Ed. LNEC. Série III, no 4.

Scotta, R., D. Trutalli, L. Marchi, L. Pozza, and M. Mirra. 2017. "Non-linear time history analyses of unreinforced masonry buildings with in-plane stiffened timber floors." 17<sup>th</sup> ANIDIS Conference, Pistoia, Italy.

Scotta, R., D. Trutalli, L. Marchi, and L. Pozza. 2018. "Seismic performance of URM buildings with in-plane non-stiffened and stiffened timber floors." *Eng. Struct.* 167, 683-694.

Scotta, R., D. Trutalli, L. Marchi, and L. Pozza. 2018. "A study about optimal stiffening of timber floors in URM buildings". 16<sup>th</sup> European Conference on Earthquake Engineering (ECEE), Thessaloniki, Greece.

Trutalli, D., L. Marchi, R. Scotta, and L. Pozza. 2017. "Dynamic simulation of an irregular masonry building with different rehabilitation methods applied to timber floors." 6<sup>th</sup> ECCOMAS Thematic Conference, Rhodes Island, Greece.

Trutalli, D., L. Marchi, R. Scotta, and L. Pozza. 2021. "Seismic capacity of irregular unreinforced masonry buildings with timber floors." Proceedings of the Institution of Civil Engineers – Structures and Buildings. <https://doi.org/10.1680/jstbu.19.00115>

Valluzzi, M. R., E. Garbin, M. Dalla Benetta, and C. Modena. 2008. "Experimental Assessment and Modelling of In-Plane Behaviour of Timber Floors." 6<sup>th</sup> International Conference on Structural Analysis of Historical Constructions, Bath, U.K., CRC-Press, Balkema, 755-762.

Valluzzi, M. R., E. Garbin, M. Dalla Benetta, and C. Modena. 2010. "In-Plane Strengthening of Timber Floors For The Seismic Improvement Of Masonry Buildings." World Conference on Timber Engineering, Riva del Garda, Italy.

Wilson, A., P. J. H. Quenneville, and J. M. Ingham. 2014. "In-plane orthotropic behavior of timber floor diaphragms in unreinforced masonry buildings." *J. Struct. Eng.* 140 (1): 04013038. [https://doi.org/10.1061/\(ASCE\)ST.1943-541X.0000819](https://doi.org/10.1061/(ASCE)ST.1943-541X.0000819).

Static scheme	Sample dimensions [mm]	Loading direction	Sample name(s)	Strengthening technique(s)
	2120×2120	Parallel to joists	<i>FM</i> (as-built); <i>FMSB</i> (as-built); <i>FM+45°SP(A)</i> ; <i>FM+45°SP(B)</i>	Overlay of planks arranged at 45° with respect to existing boards (Valluzzi et al. 2008; Valluzzi et al. 2010)
	3000×3000	Parallel to joists	<i>01-T2-OR</i> (as-built); <i>02-T6-OR</i> (as-built); <i>03-T4-T6</i>	Overlay of planks arranged at 90° with respect to existing boards (Corradi et al. 2006)
	2125×2125	Parallel to joists	<i>S</i> (as-built); <i>SS</i>	Overlay of planks arranged at 90° with respect to existing boards (Branco et al. 2015)
	3160×3000	Parallel to joists	<i>UR-2</i> (as-built); <i>OSB90-R-2</i> ; <i>OSB0-S-2</i>	Overlay of OSB panels arranged parallel or perpendicular to joists (Gubana and Melotto 2018)
	7320×3660	Parallel to joists	<i>MAE-2</i> (as-built); <i>MAE-2B</i> ; <i>MAE-2C</i>	Overlay of plywood panels (Peralta et al. 2004)
	4000×3000	Parallel to joists	<i>AB-1</i> (as-built); <i>R-1</i>	Overlay of plywood panels (Brignola et al. 2012)
	9600×4700	Orthogonal to joists	<i>26_B_asB</i> (as-built); <i>35_B_Plyw</i>	Overlay of plywood panels (Giongo et al. 2013)

**Fig. 1.** Overview of the timber diaphragms examined in the present work. For visual comparison, the static schemes are reported at the same scale, along with in-plane deformed shapes and drifts  $\gamma$ . The first given dimension is always the one orthogonal to the load; sample names are reported according to the Authors' nomenclature.

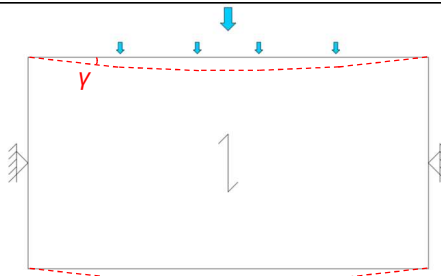
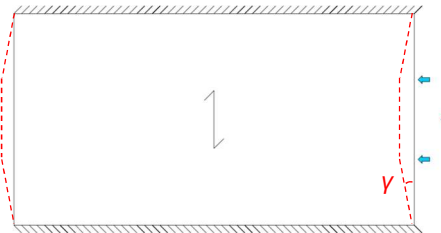
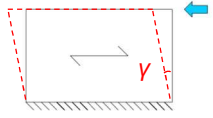
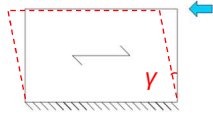
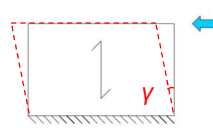
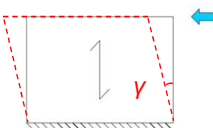
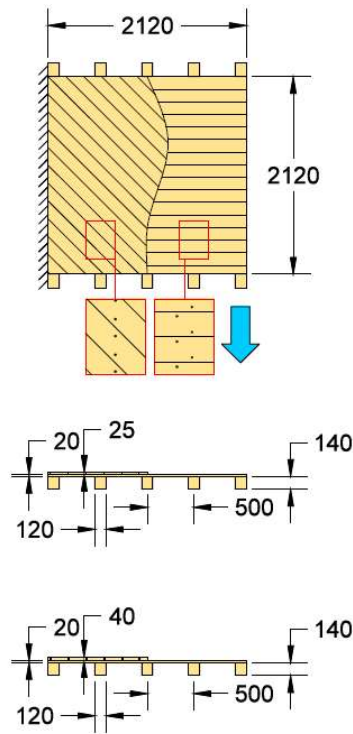
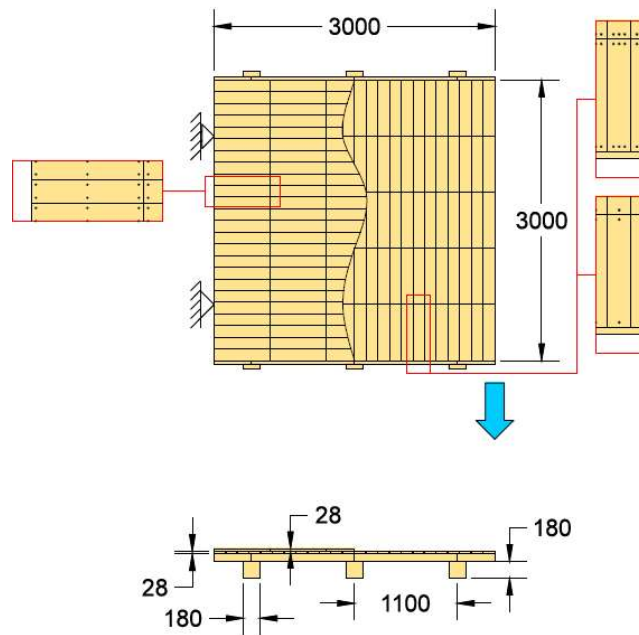
Static scheme	Sample dimensions [mm]	Loading direction	Sample name(s)	Strengthening technique(s)
	10400×5500	Parallel to joists	1a-PARA (as-built); 1b-PARA	Overlay of plywood panels (Wilson et al. 2014)
	5500×10400	Orthogonal to joists	1a-PERP (as-built); 1b-PERP	Overlay of plywood panels (Wilson et al. 2014)
	2400×3800	Parallel to joists	DFpar-1 (as-built); DFpar-1s	Overlay of plywood panels (Mirra et al. 2020)
	2400×3960	Parallel to joists	DFpar-2 (as-built); DFpar-2s	Overlay of plywood panels (Mirra et al. 2020)
	2300×3800	Orthogonal to joists	DFper-3 (as-built); DFper-4 (as-built); DFper-3s; DFper-4s	Overlay of plywood panels (Mirra et al. 2020)
	2730×3800	Orthogonal to rafters	DRpar-5 (as-built); DRpar-5s	Overlay of plywood panels (Mirra et al. 2020)

Fig. 1 (continued).



**Fig. 2.** Floor tested by Valluzzi et al. (2008) and Valluzzi et al. (2010). The two cross-sections show the different methods for strengthening the diaphragm: thin straight-edged planks (*FM+45°SP(A)*, top) or thick tongue-and-groove ones (*FM+45°SP(B)*, bottom). All dimensions are given in mm



**Fig. 3.** Floor tested by Corradi et al. (2006); dimensions in mm

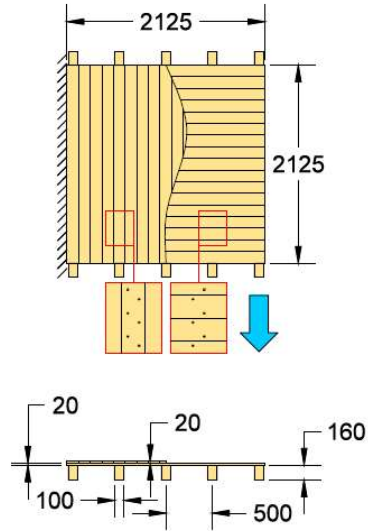


**Fig. 4.** Floor tested by Branco et al. (2015); dimensions in mm.

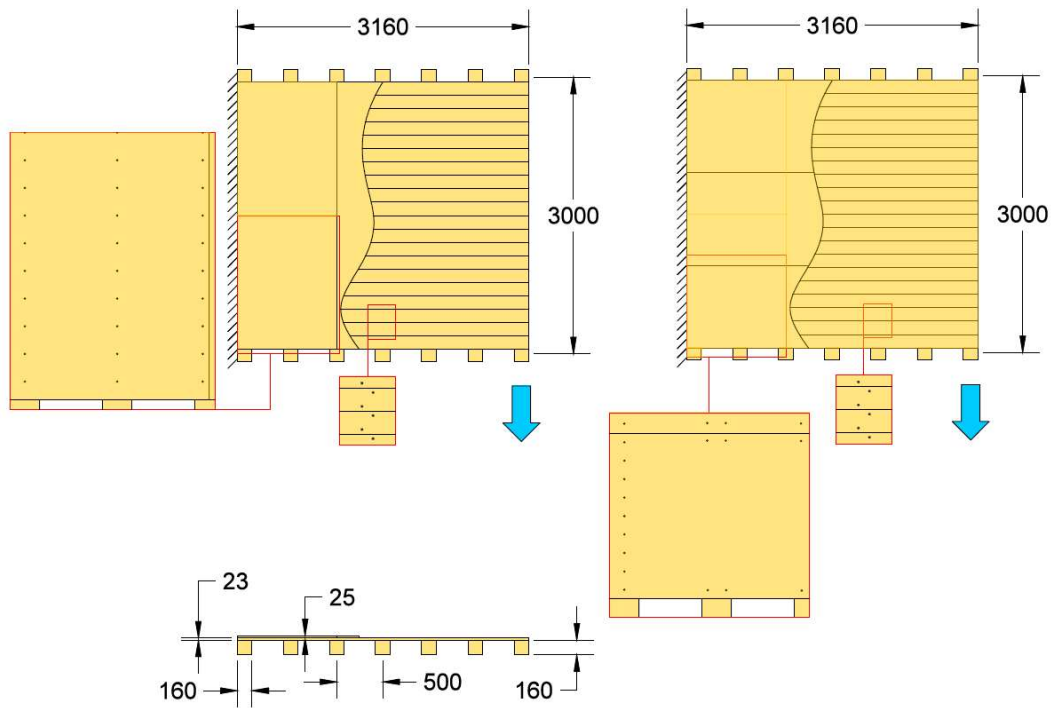


**Fig. 5.** Floor tested by Gubana and Melotto (2018); the two retrofitting options are shown, with OSB panels arranged parallel or perpendicular to joists. Dimensions in mm.

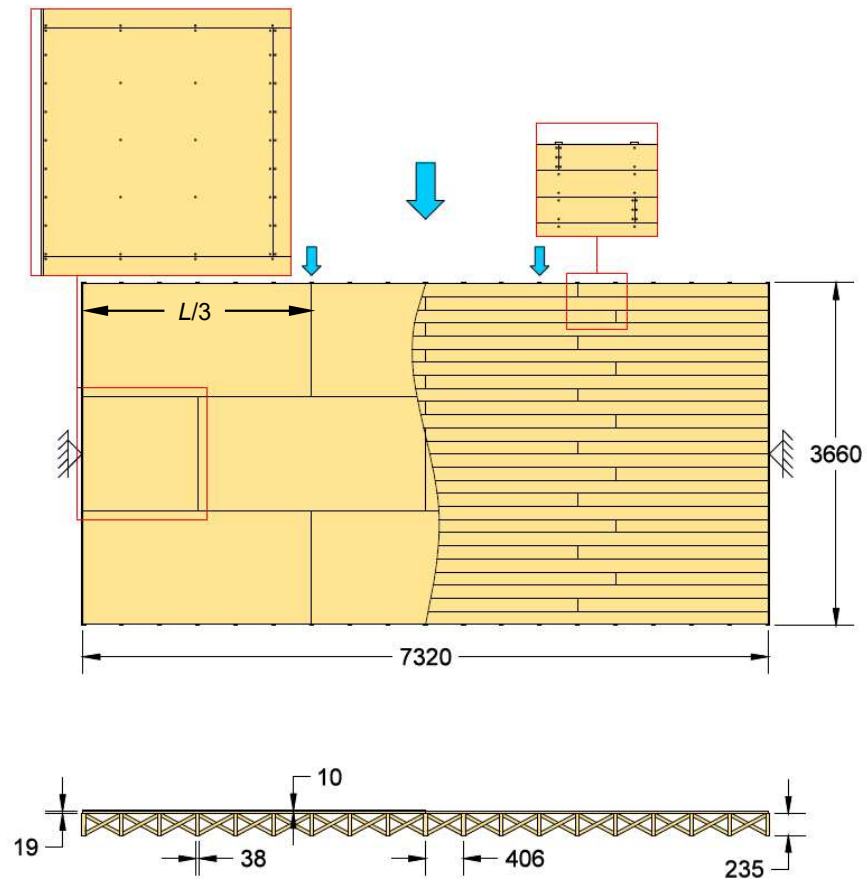


**Fig. 6.** Floor tested by Peralta et al. (2004); dimensions in mm

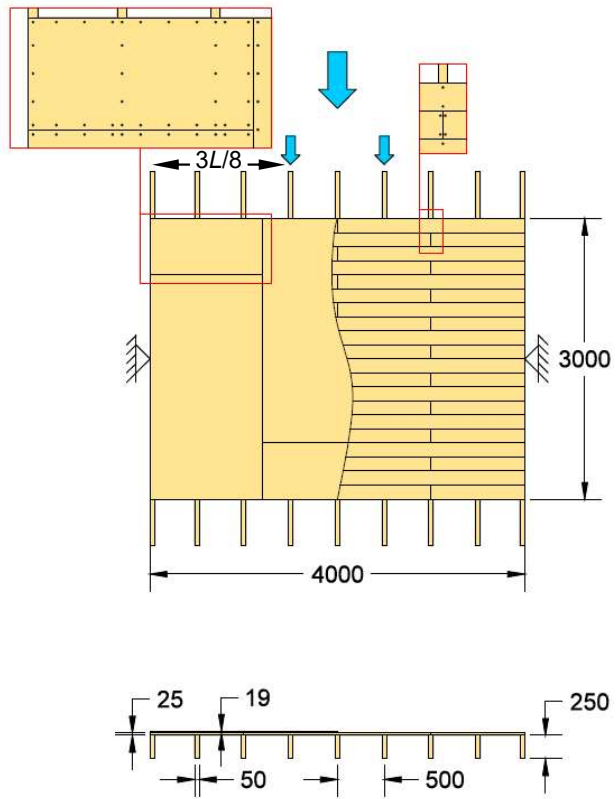


**Fig. 7.** Floor tested by Brignola et al. (2012); dimensions in mm

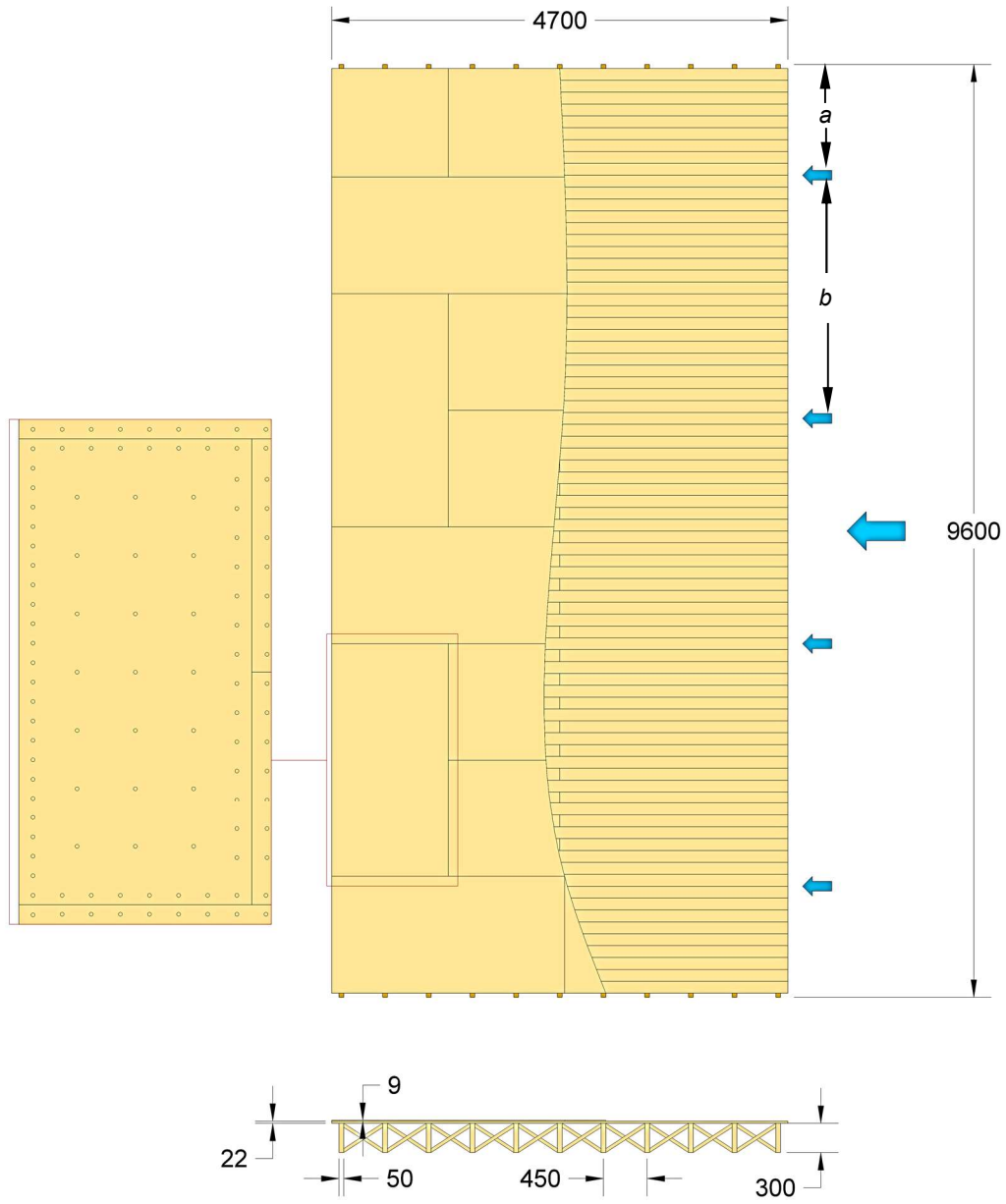


**Fig. 8.** Floor tested by Giongo et al. (2013); dimensions in mm

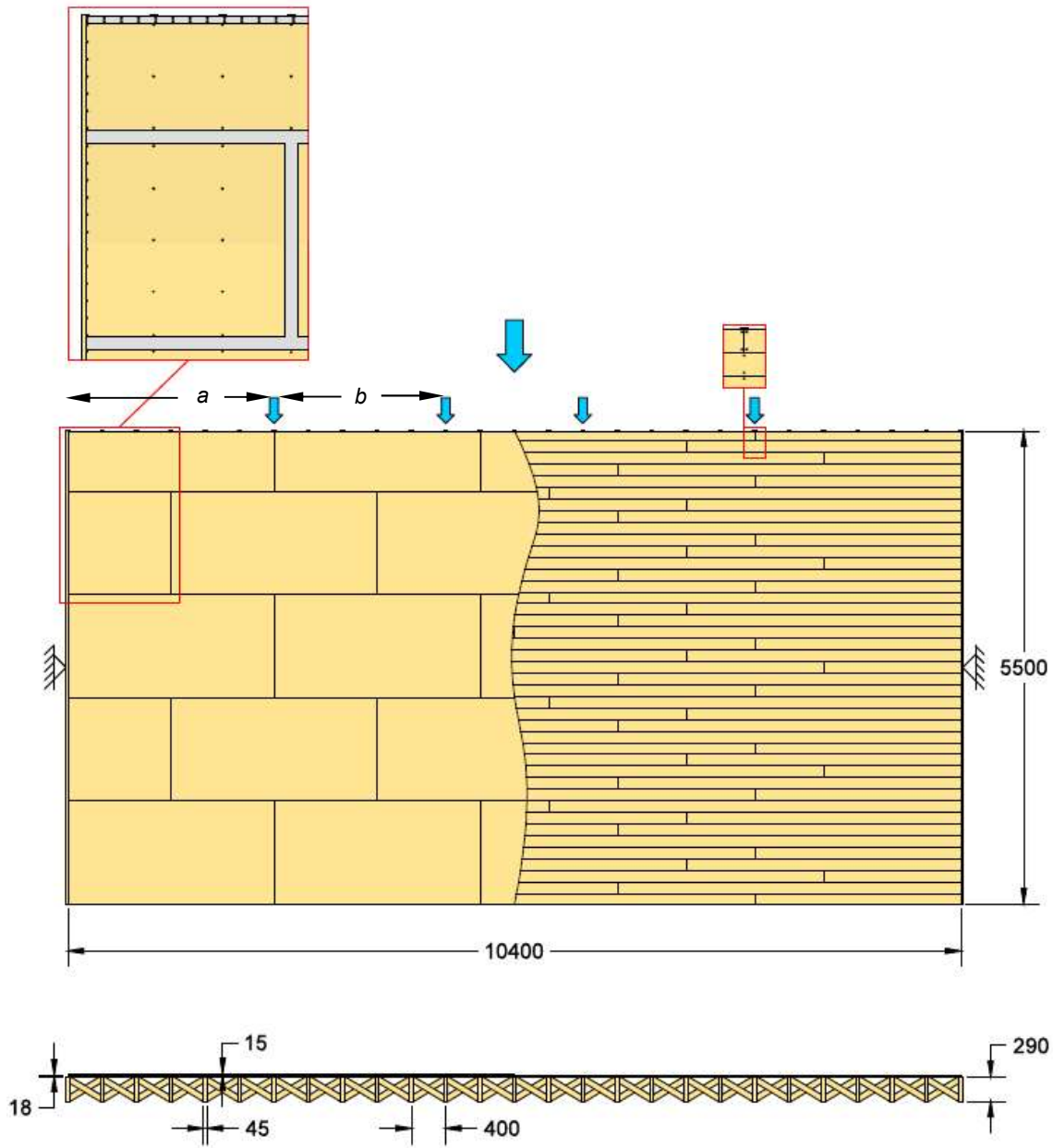


**Fig. 9.** Floor tested by Wilson et al. (2014), direction parallel to main joists (*1a-PARA* and *1b-PARA*); dimensions in mm

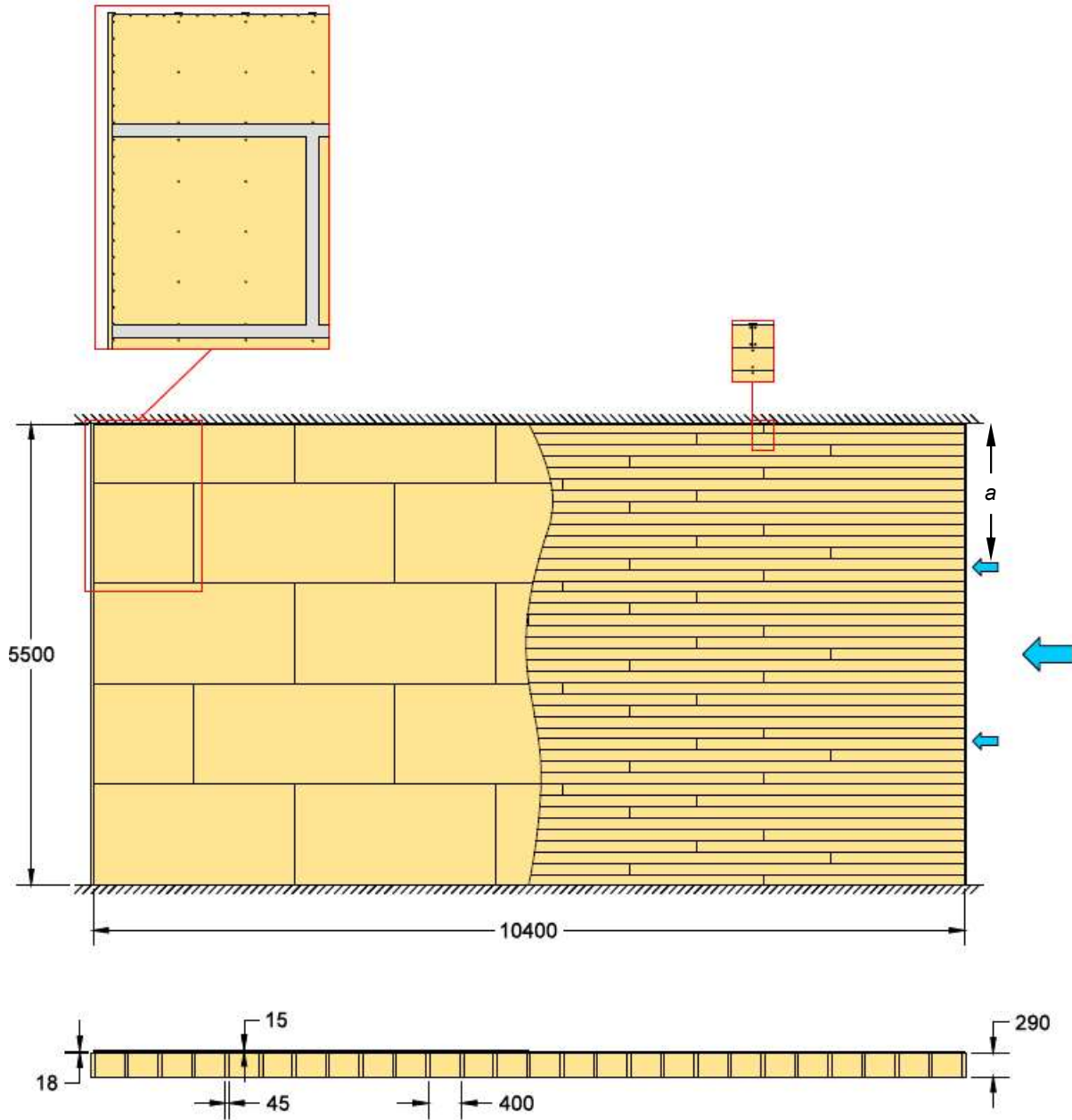


**Fig. 10.** Floor tested by Wilson et al. (2014), direction orthogonal to the joist (*1a-PERP* and *1b-PERP*); dimensions in mm

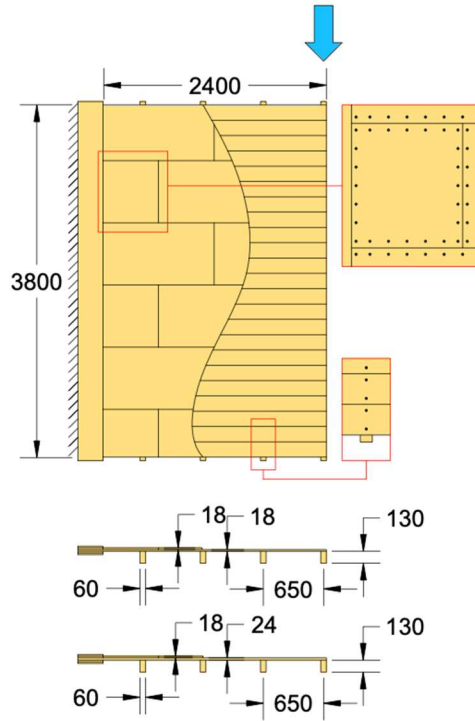


**Fig. 11.** Specimens *DFpar-1(s)* (upper cross-section) and *DFpar-2(s)* (lower cross-section) (Mirra et al. 2020). Long side measured 3960 mm for sample *DFpar-2(s)*; dimensions in mm

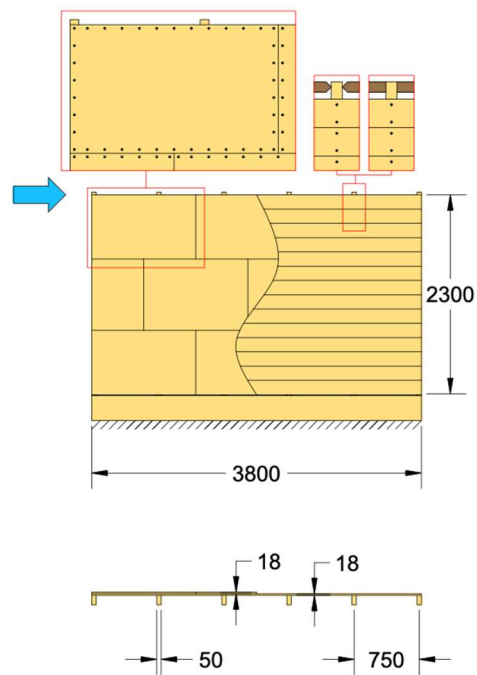


**Fig. 12.** Specimens *DFper-3(s)* (hinged) and *DFper-4(s)* (clamped) (Mirra et al. 2020); dimensions in mm

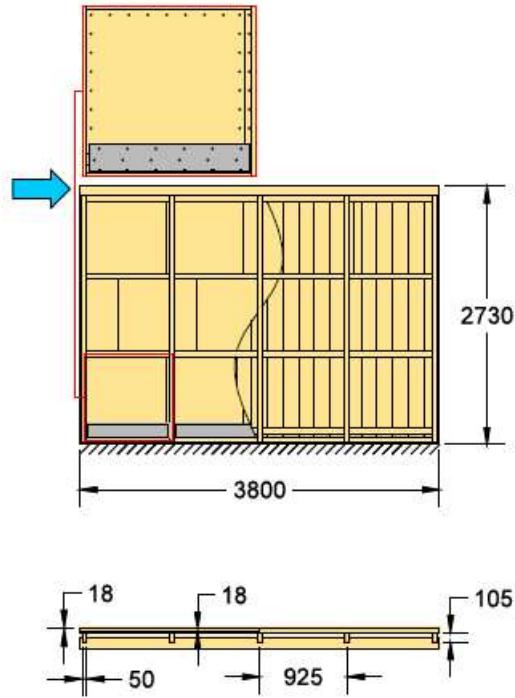


**Fig. 13.** Specimen *DRpar-5(s)*, representing a roof pitch (Mirra et al. 2020); dimensions in mm

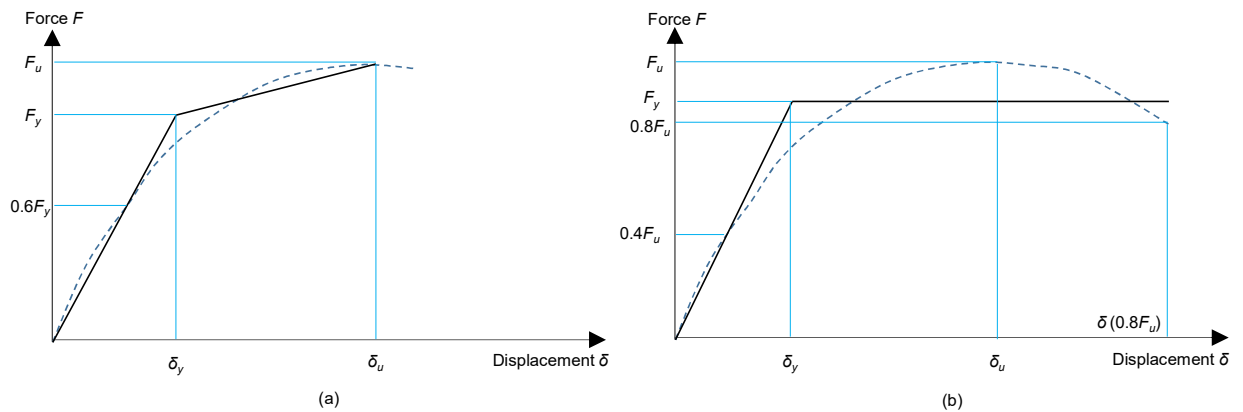


**Fig. 14.** Bilinear methods for schematizing the experimentally obtained backbone curves: (a) procedure according to FEMA guidelines (FEMA 273 1997, FEMA 356 2000), (b) elasto-plastic bilinearization according to ASTM E 2126 (2019); both methods are based on the principle of the energy equivalence between the two curves.

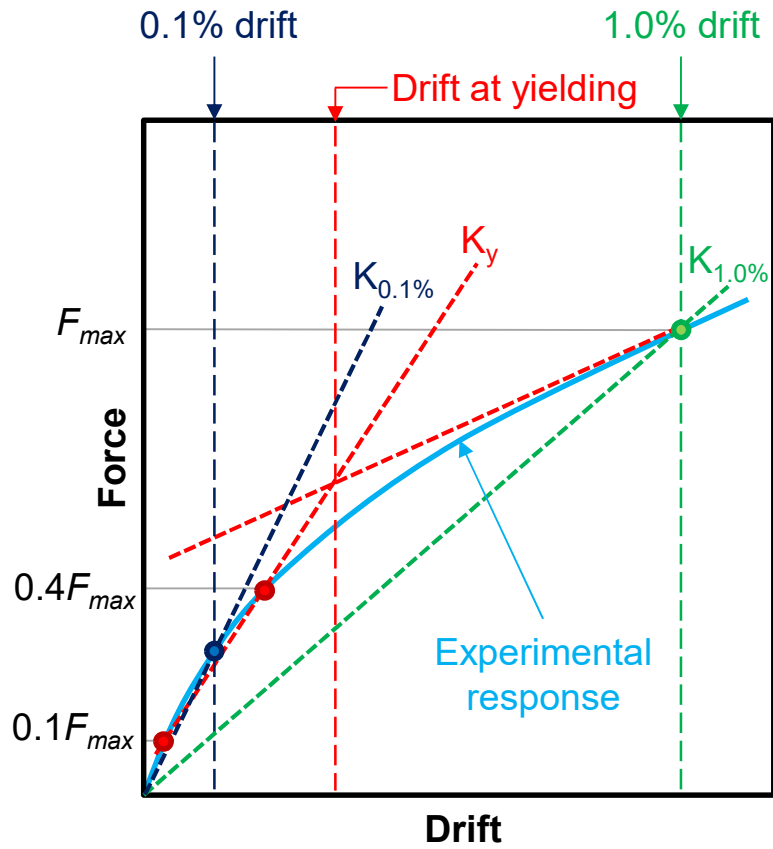
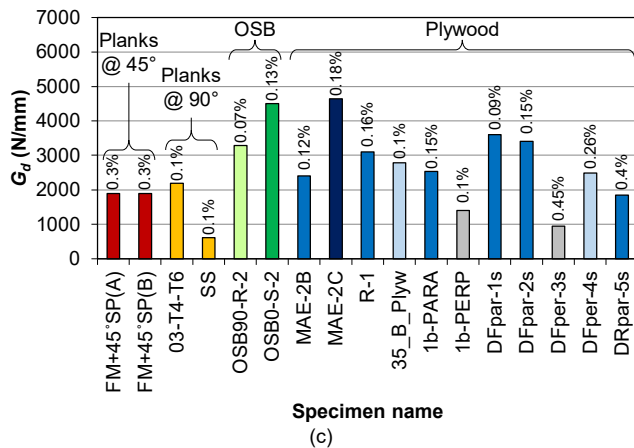
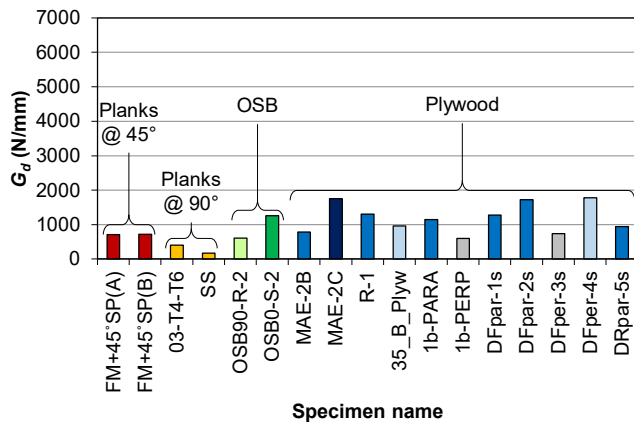
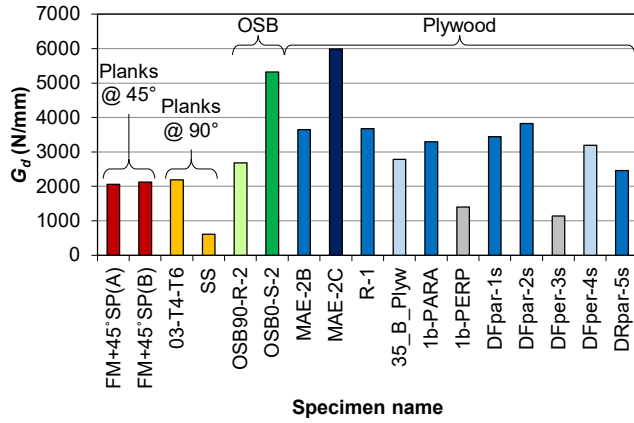


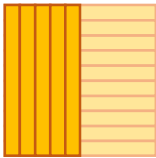
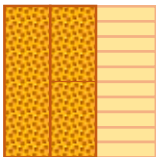
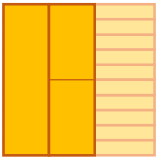
**Fig. 15.** Derivation of the stiffness  $K$  at different drift levels: 0.1%, 1.0% and at a conventional yielding point, defined as the intersection between an initial stiffness determined according to EN 12512 (2001), and the tangent to the experimental curve at 1.0% drift.



**Legend**

- Strengthening with a superposition of planks arranged at angle of 45° with respect to the original sheathing
- Strengthening with a superposition of planks arranged at angle of 90° with respect to the original sheathing
- Strengthening with an overlay of OSB panels positioned perpendicular to the joists
- Strengthening with an overlay of OSB panels positioned parallel to the joists
- Strengthening with an overlay of plywood panels (loading parallel to the joists)
- Strengthening with an overlay of blocked plywood panels (loading parallel to the joists)
- Strengthening with an overlay of plywood panels (loading perpendicular to the joists)
- Strengthening with an overlay of blocked plywood panels (loading perpendicular to the joists)

**Fig. 16.** Comparison of the equivalent shear stiffness of strengthened diaphragms at 0.1% (a) and 1.0 % (b) drift, and at yielding (c); in the latter case the corresponding drift is also indicated. The retrofitting techniques are identified by groups, and colors identify specific strengthening characteristics.

Strengthening method		$G_d$ [N/mm]		
		0.1% drift	1.0% drift	Yielding
	<b>Overlay of planks at 45°</b>			
	Traditional floors Useful correlations: $G_{d,1.0\%} \approx G_{d,0.1\%}/3$	2000	700	1900
	<b>Overlay of planks at 90°</b>			
	Floors with double warping (main and secondary joists) Traditional floors Useful correlations: $G_{d,1.0\%} \approx G_{d,0.1\%}/3.5$	2200 600	400 170	2200 600
	<b>OSB panels overlay</b>			
	Panels parallel to joists Panels orthogonal to joists Useful correlations: $G_{d,1.0\%} \approx G_{d,0.1\%}/4.5$ $G_{d,\perp} \approx G_{d,\parallel}/2$	5300 2700	1200 600	4500 3300
	<b>Plywood panels overlay</b>			
	Loading parallel to joists Loading orthogonal to joists: - Without blocking at floor edge - With blocking at floor edge Fully blocked panels Useful correlations: $G_{d,\parallel,1.0\%} \approx G_{d,\parallel,0.1\%}/2.5$ $G_{d,\perp,1.0\%} \approx G_{d,\perp,0.1\%}/2$ (no blocking) $G_{d,\perp} \approx G_{d,\parallel}$ (edge blocking) $G_{d,\perp} \approx G_{d,\parallel}/2.5$ (no blocking) $G_{d,unblocked} \approx G_{d,blocked}/1.5$	3400 1300 3400 6000	1300 700 1300 1700	2800 1200 2800 4600

**Fig. 17.** Average values of in-plane stiffness of the strengthened diaphragms from the compared data. The symbols parallel and perpendicular in the subscript of  $G_d$  refer to the loading direction with respect to the joists.

**Table 1.** Overview of in-plane stiffness values for as-built and strengthened timber diaphragms. Values of equivalent shear stiffness that are size-dependent because of the flexural properties of as-built floors are reported in italic.

Authors	Standards adopted by Authors for stiffness evaluation	Sample names	K [kN/mm]				G <sub>d</sub> [N/mm]			
			From Authors	0.1% drift	1.0% drift	Yielding (drift)	From Authors	0.1% drift	1.0% drift	Yielding (drift)
Valluzzi et al. (2008); Valluzzi et al. (2010)	EN 12512, with $F_{max}$ at 30 mm displacement	<i>FMSB (F1.M)</i> (O)	0.08	0.15	0.04	0.1 (0.12%)	81	152	43	100 (0.12%)
		<i>FM (F2.M)</i> (O)	0.29	0.31	0.06	0.33 (0.12%)	288	313	62	330 (0.12%)
		<i>FM+45°SP(A)</i> (S)	1.18	2.06	0.71	1.89 (0.3%)	1176	2065	707	1890 (0.3%)
		<i>FM+45°SP(B)</i> (S)	1.25	2.13	0.72	1.89 (0.3%)	1247	2128	719	1890 (0.3%)
Corradi et al. (2006)	ASTM E 519-81	<i>01-T2-OR</i> (O)	0.47	0.71	0.13	0.23 (0.07%)	470	710	128	230 (0.07%)
		<i>02-T6-OR</i> (O)	0.28	0.77	0.20	0.26 (0.08%)	280	771	204	255 (0.08%)
		<i>03-T4-T6</i> (S)	1.71	2.19	0.40	2.19 (0.1%)	1710	2190	400	2190 (0.1%)
Branco et al. (2015)	EN 12512, with $F_{max}$ at 100 mm displacement	<i>S</i> (O)	0.05	0.15	0.05	0.16 (0.14%)	55	153	53	165 (0.14%)
		<i>SS</i> (S)	0.13	0.61	0.16	0.61 (0.1%)	132	609	165	609 (0.1%)
Gubana and Melotto (2018)	EN 12512 as such	<i>UR-2</i> (O)	0.53	0.55	0.09	0.55 (0.1%)	560	582	97	582 (0.1%)
		<i>OSB90-R-2</i> (S)	1.77	2.55	0.57	3.12 (0.07%)	1870	2691	606	3290 (0.07%)
		<i>OSB0-S-2</i> (S)	1.97	5.05	1.19	4.27 (0.13%)	2080	5320	1259	4496 (0.13%)
Peralta et al. (2004)	FEMA 273, FEMA 356	<i>MAE-2</i> (O)	1.80	5.84	1.42	5.84 (0.1%)	600	1949	475	1949 (0.1%)
		<i>MAE-2B</i> (S)	8.40	10.96	2.34	7.76 (0.12%)	2800	3653	780 <sup>(a)</sup>	2400 (0.12%)
		<i>MAE-2C</i> (S)	11.30	17.96	5.22	13.93 (0.18%)	3767	5990	1743 <sup>(a)</sup>	4644 (0.18%)
Brignola et al. (2012)	None, secant stiffness calculation at 12 mm displacement	<i>AB-1</i> (O)	1.36	3.06	1.16	3.02 (0.18%)	340	769	290	756 (0.18%)
		<i>R-1</i> (S)	6.65	14.70	5.20	12.40 (0.16%)	1665	3675	1300	3102 (0.16%)
Giongo et al. (2013)	None, secant stiffness calculation at various drifts	<i>26_B_asB</i> (O)	-	1.16	0.65	1.00 (0.25%)	190	302	169	260 (0.25%)
		<i>35_B_Plyw</i> (S)	-	10.70	3.69	10.70 (0.1%)	1343	2783	961	2783 (0.1%)
Wilson et al. (2014)	FEMA 273, FEMA 356, ASTM E 2126	<i>1a-PARA</i> (O)	0.64	2.06	0.47	2.06 (0.1%)	198	637	148	637 (0.1%)
		<i>1b-PARA</i> (S)	14.52	19.55	3.66	15.00 (0.15%)	4459	3294	1140	2533 (0.15%)
		<i>1a-PERP</i> (O)	1.61	5.34	1.54	3.75 (0.14%)	134	441	128	313 (0.14%)
		<i>1b-PERP</i> (S)	22.41	30.89	7.15	30.89 (0.1%)	1864	1402	595	1402 (0.1%)
Mirra et al. (2020)	None, secant stiffness calculation at various drifts	<i>DFpar-1</i> (O)	-	0.74	0.36	0.48 (0.28%)	-	467	227	303 (0.28%)
		<i>DFpar-2</i> (O)	-	0.86	0.47	0.57 (0.16%)	-	521	285	345 (0.16%)
		<i>DFper-3</i> (O)	-	0.33	0.11	0.25 (0.15%)	-	200	67	151 (0.15%)
		<i>DFper-4</i> (O)	-	0.21	0.10	0.21 (0.1%)	-	127	60	127 (0.1%)
		<i>DRpar-5</i> (O)	-	0.15	0.06	0.15 (0.1%)	-	108	41	108 (0.1%)
		<i>DFpar-1s</i> (S)	-	5.45	2.02	5.70 (0.09%)	-	3441	1277	3600 (0.09%)
		<i>DFpar-2s</i> (S)	-	6.32	2.83	5.61 (0.15%)	-	3832	1717	3403 (0.15%)
		<i>DFper-3s</i> (S)	-	1.88	1.21	1.56 (0.45%)	-	1136	735	946 (0.45%)
		<i>DFper-4s</i> (S)	-	5.28	2.93	4.11 (0.26%)	-	3196	1773	2488 (0.26%)
		<i>DRpar-5s</i> (S)	-	3.42	1.31	2.57 (0.4%)	-	2457	940	1848 (0.4%)

<sup>(a)</sup> Values obtained from an extrapolation of the experimental curve and not directly from it, because the test was stopped slightly before reaching this drift value.